

2-hydroxyglutarate detection by magnetic resonance spectroscopy in subjects with IDH-mutated gliomas

Changho Choi^{1,2}, Sandeep K Ganji^{1,2}, Ralph J DeBerardinis³⁻⁵, Kimmo J Hatanpaa⁵⁻⁷, Dinesh Rakheja^{6,8}, Zoltan Kovacs¹, Xiao-Li Yang^{5,7,9}, Tomoyuki Mashimo^{5,7,9}, Jack M Raisanen⁵⁻⁷, Isaac Marin-Valencia³, Juan M Pascual^{3,10,11}, Christopher J Madden^{5,7,12}, Bruce E Mickey^{5,7,12}, Craig R Malloy^{1,2,9,13}, Robert M Bachoo^{5,7,9,10} & Elizabeth A Maher^{5,7,9,10}

Mutations in isocitrate dehydrogenases 1 and 2 (IDH1 and IDH2) have been shown to be present in most World Health Organization grade 2 and grade 3 gliomas in adults. These mutations are associated with the accumulation of 2-hydroxyglutarate (2HG) in the tumor. Here we report the noninvasive detection of 2HG by proton magnetic resonance spectroscopy (MRS). We developed and optimized the pulse sequence with numerical and phantom analyses for 2HG detection, and we estimated the concentrations of 2HG using spectral fitting in the tumors of 30 subjects. Detection of 2HG correlated with mutations in IDH1 or IDH2 and with increased levels of D-2HG by mass spectrometry of the resected tumors. Noninvasive detection of 2HG may prove to be a valuable diagnostic and prognostic biomarker.

Isocitrate dehydrogenase converts isocitrate to α -ketoglutarate (α KG) in the cytosol (IDH1) and mitochondria (IDH2). The recent identification of mutations in IDH1 and IDH2 among most humans with World Health Organization (WHO) grade 2 and 3 gliomas^{1,2} has directed attention to the role of abnormal metabolism in the pathogenesis and progression of these primary brain tumors. The mutations are confined to the active site of the enzyme and result in a gain of function that generates 2HG (ref. 3) and induces DNA hypermethylation^{4,5}. The abundance of this metabolite, normally present in vanishingly small quantities, can be elevated by orders of magnitude in gliomas with IDH1 or IDH2 mutations. Intracellular concentrations on the order of several micromoles per gram of tumor have been reported³.

Although the metabolic consequences and downstream molecular effects of these mutations are yet to be elucidated, their potential value as diagnostic and prognostic markers in gliomas has been established from their clear association with improved overall survival when outcomes are compared between IDH-mutated and IDH wild-type

tumors^{2,6}. Immunohistochemistry with a commercially available antibody to the R132H mutation of *IDH1* identifies approximately 93% of the mutations, but the remaining 7% of tumors carrying a different *IDH1* or an *IDH2* mutation require direct sequencing for detection⁷. As 2HG is produced by all known *IDH*-mutant enzymes, evaluation of 2HG abundance is an alternative indirect method for determining IDH status. The finding that 2HG is present at high levels in IDHmutated gliomas has raised the possibility that this metabolite could be detected noninvasively by MRS. Brain magnetic resonance imaging is the primary modality for clinical evaluation of people with gliomas, so the ability to detect 2HG by MRS could provide important diagnostic and prognostic information.

Here we report the noninvasive detection of 2HG in glioma in vivo by MRS at 3 tesla (T). We optimized the point-resolved spectroscopy (PRESS)⁸ and difference editing⁹ sequences with quantum-mechanical and phantom analyses for detection of 2HG in the human brain and applied them to tumor masses in 30 adults with all grades of gliomas. Analysis of MRS data was blinded to IDH status. For each case in which 2HG was detected by MRS, we confirmed an IDH1 or IDH2 mutation in the tumor. Failure to detect 2HG by MRS was associated with the detection of wild-type IDH1 and IDH2 in each case. The sensitivity and specificity of the method described here and the ease with which it could be incorporated into standard magnetic resonance imaging suggests that 2HG detection by MRS may be an important biomarker in the clinical management of these patients.

RESULTS

Optimization of MRS methods

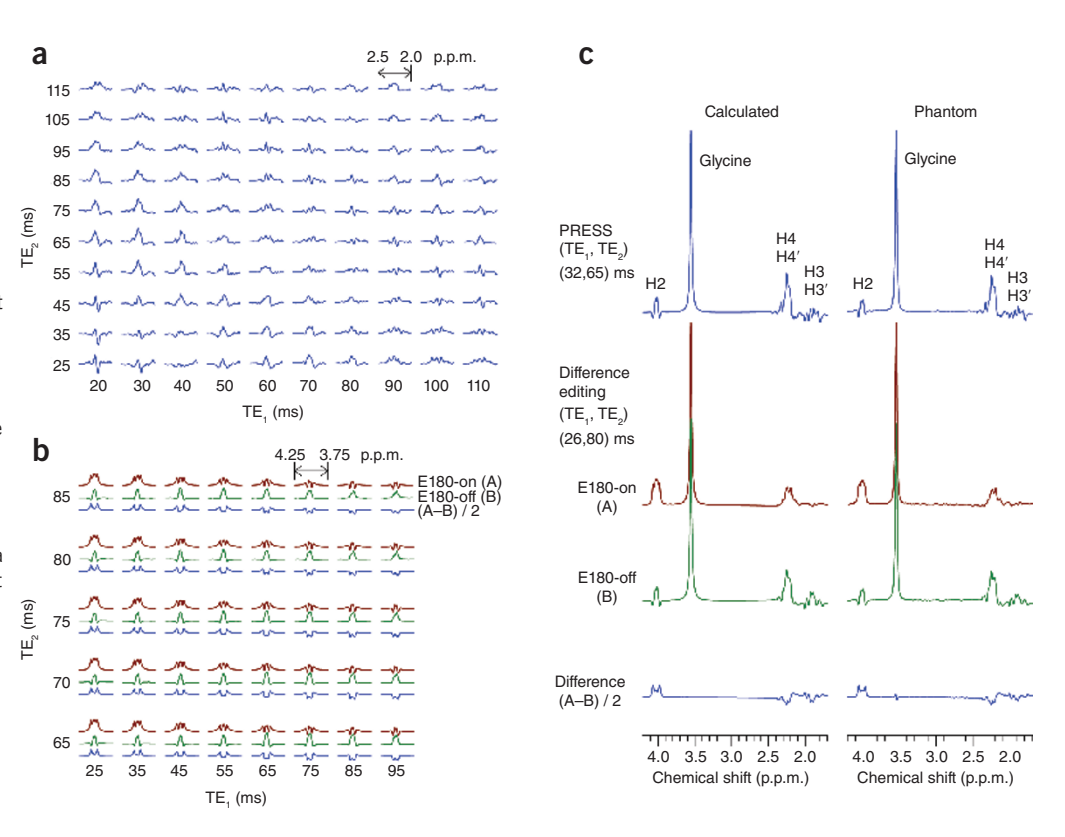
A 2HG molecule has five nonexchangeable scalar-coupled protons, resonating at 4.02 p.p.m., 2.27 p.p.m., 2.22 p.p.m., 1.98 p.p.m. and 1.83 p.p.m.¹⁰, giving rise to multiplets at approximately three locations at 3 T; that is, 4.02 p.p.m. (H2), ~2.25 p.p.m. (H4 and H4') and ~1.9 p.p.m.

¹Advanced Imaging Research Center, University of Texas Southwestern Medical Center, Dallas, Texas, USA. ²Department of Radiology, University of Texas Southwestern Medical Center, Dallas, Texas, USA. 3Department of Pediatrics, University of Texas Southwestern Medical Center, Dallas, Texas, USA. 4McDermott Center for Human Growth and Development, University of Texas Southwestern Medical Center, Dallas, Texas, USA. 5Harold C. Simmons Cancer Center, University of Texas Southwestern Medical Center, Dallas, Texas, USA. ⁶Department of Pathology, University of Texas Southwestern Medical Center, Dallas, Texas, USA. ⁷Annette Strauss Center for Neuro-Oncology, University of Texas Southwestern Medical Center, Dallas, Texas, USA. 8Children's Medical Center, Dallas, Texas, USA. 9Department of Internal Medicine, University of Texas Southwestern Medical Center, Dallas, Texas, USA. 10Department of Neurology and Neurotherapeutics, University of Texas Southwestern Medical Center, Dallas, Texas, USA. 11Department of Physiology, University of Texas Southwestern Medical Center, Dallas, Texas, USA. 12Department of Neurological Surgery, University of Texas Southwestern Medical Center, Dallas, Texas, USA. ¹³Veterans Affairs North Texas Health Care System, Dallas, Texas, USA. Correspondence should be addressed to C.C. (changho.choi@utsouthwestern.edu) or E.A.M. (elizabeth.maher@utsouthwestern.edu).

Received 26 April 2011; accepted 17 August 2011; published online 26 January 2012; corrected online 31 January 2012 (details online); doi:10.1038/nm.2682



Figure 1 Theoretical and experimental spectra of 2HG. (a) Quantum-mechanically calculated spectra of the 2HG H4 resonances, at 3 T, are plotted against TE₁ and TE2 of PRESS (subecho times of the first slice- and second sliceselective 180° radiofrequency pulses, respectively). (b) Calculated difference-edited multiplets of the 2HG H2 resonance are plotted against subecho times TE_1 and TE_2 of scalar difference editing. Shown for each TE₁-TE₂ pair are, top to bottom, E180-on (brown) and E180-off (green) subspectra, and the difference between the two subspectra (blue). Here, E180 denotes editing 180° pulses tuned to 1.9 p.p.m. PRESS and edited spectra are all broadened to a singlet line width of 4 Hz. Spectra in a and b are scaled equally for direct comparison. Relaxation effects were not included in the calculations. (c) Calculated and phantom spectra of 2HG for PRESS and difference editing. The echo times were 97 ms and 106 ms for PRESS and editing. The concentrations of 2HG and glycine in the phantom were both 10 mM (pH = 7.0). Spectra are scaled with respect to the glycine singlet at 3.55 p.p.m.



(H3 and H3') (Supplementary Fig. 1). The 2HG resonances are all scalar coupled, and, consequently, the spectral pattern and signal strength vary with changing echo time of MRS sequence. A maximum 2HG signal may be expected at ~2.25 p.p.m. where the H4 and H4' spins resonate proximately to each other. Because of its capability of full refocusing, in the present study we used a PRESS sequence as a major tool for 2HG measurement.

We conducted quantum mechanical simulations to search for optimal experimental parameters. The simulation indicated that the 2HG H4 resonances give rise to a maximum multiplet at total echo time of 90-100 ms, for which the first subecho time, TE₁, is shorter than the second subecho time, TE₂ (Fig. 1a). Given the large spectral distance of the H2 resonance from its weak coupling partners (H3 spins), we also measured the H2 resonance by means of difference editing. Selective 180° rotation of the H3 spins was switched on and off within a PRESS sequence in alternate scans to induce unequal H2 multiplets in subspectra. Subtraction between the spectra generated an edited 2HG H2 multiplet, canceling other resonances that were not affected by the editing 180° pulses. The computer simulation indicated that a large edited H2 signal can be obtained using a short-echo-time set in which TE₁ should be the shortest possible (Fig. 1b). We optimized the subecho times of the PRESS and difference editing sequences to (TE₁, TE₂) = (32, 65) ms and (26, 80) ms, respectively. We tested these optimized MRS sequences in an aqueous solution with 2HG that was synthesized in house. The spectral pattern and signal intensity of 2HG were consistent between calculation and experiment (Fig. 1c).

The optimized PRESS provided a 2HG multiplet at approximately 2.25 p.p.m. with maximum amplitude among echo times greater than 40 ms (Supplementary Fig. 2a,b). Moreover, the optimized echo time gave rise to narrowing of the multiplet and substantial reduction of 2HG signals at approximately 1.9 p.p.m. Similar signal modulation

occurred in the glutamate multiplets, allowing 2HG to be measured with high selectivity against the background signals of adjacent resonances (Supplementary Fig. 2c,d). The optimized echo time is relatively long, so signal loss due to transverse relaxation effects may be considerable in vivo. However, given that 2HG does not have a welldefined spectral pattern at short echo times (for example, 30 ms), the 2HG signals can be better resolved at the optimized long echo time, benefiting from the suppressed complex baseline signals of macromolecules. The signal yield of 2HG in difference editing was low (38%) compared to that in PRESS (Fig. 1), but the editing provides a useful tool for proving 2HG elevation because the edited signal at 4.02 p.p.m. is uniquely generated via the coupling connections of 2HG. In vivo, because the difference editing uses spectral difference induced by selective 180° rotations tuned at approximately 1.9 p.p.m., the 4.15-p.p.m. resonance of the glutamate moiety of N-acetylaspartylglutamate¹¹ is co-edited, but the resonance is relatively distant from the 2HG 4.02-p.p.m. resonance and thus does not interfere with 2HG editing (**Supplementary Fig. 3**). The lactate resonance at 4.1 p.p.m.¹² is not co-edited because the coupling partners at 1.31 p.p.m. are not influenced by the editing 180° pulse.

For spectral fitting, in the present study we used model spectra that were calculated including the effects of the volume-localized radiofrequency pulses used for in vivo measurements, allowing spectral fitting by signal patterns identical to those obtained by experiment. Calculation of spectra at numerous echo times for MRS sequence optimization was efficiently accomplished using the product operator-based transformation-matrix algorithm in the quantum-mechanical simulations $^{13-15}$ (Supplementary Methods). The spectral pattern of 2HG is pH depen $dent^{10}$, with large shifts noted for pH < 6 (Supplementary Fig. 4). We performed computer simulations and MRS sequence optimization for 2HG detection assuming pH \sim 7.0 in tumors^{16–18}.

Table 1 Correlation between 2HG detection by MRS PRESS and IDH1 and IDH2 mutational status

Histological diagnosis	2HG by MRS (mM (CRLB))	IDH1 and IDH2 mutations by DNA sequencing	IDH1 R132H by immunohistochemistry
Oligodendroglioma (WHO grade 2)	3.3 (11%)	<i>IDH1</i> (R132H)	Positive
Oligodendroglioma (WHO grade 2)	2.6 (14%)	IDH1 (R132C)	Negative
Oligodendroglioma (WHO grade 2)	1.7 (17%)	<i>IDH1</i> (R132H)	Positive
Oligodendroglioma (WHO grade 2)	3.3 (7%)	IDH1 (R132C)	Negative
Astrocytoma (WHO grade 2)	4.2 (10%)	<i>IDH1</i> (R132H)	Positive
Astrocytoma (WHO grade 3)	2.1 (16%)	<i>IDH1</i> (R132H)	Positive
Oligoastrocytoma (WHO grade 3)	3.9 (6%)	<i>IDH1</i> (R132H)	Positive
Oligodendroglioma (WHO grade 3)	8.9 (3%)	<i>IDH1</i> (R132H)	Positive
Oligoastrocytoma (WHO grade 3)	3.4 (8%)	<i>IDH2</i> (R172W)	Negative
Astrocytoma (WHO grade 3)	2.7 (11%)	IDH2 (R172G)	Negative
Astrocytoma (WHO grade 3)	5.3 (6%)	<i>IDH1</i> (R132H)	Positive
Astrocytoma (WHO grade 3)	2.5 (16%)	IDH1 (R132C)	Negative
Astrocytoma (WHO grade 3)	2.2 (15%)	IDH1 (R132C)	Negative
Astrocytoma (WHO grade 3)	ND	None	Negative
Secondary glioblastoma (WHO grade 4)	2.1 (15%)	<i>IDH1</i> (R132H)	Positive
Glioblastoma (WHO grade 4)	ND	None	Negative
Glioblastoma (WHO grade 4)	ND	None	Negative
Glioblastoma (WHO grade 4)	ND	None	Negative
Glioblastoma (WHO grade 4)	ND	None	Negative
Glioblastoma (WHO grade 4)	ND	None	Negative
Glioblastoma (WHO grade 4)	ND	None	Negative
Glioblastoma (WHO grade 4)	ND	None	Negative
Glioblastoma (WHO grade 4)	ND	None	Negative
Glioblastoma (WHO grade 4)	ND	None	Negative
Glioblastoma (WHO grade 4)	ND	None	Negative
Glioblastoma (WHO grade 4)	ND	None	Negative
Glioblastoma (WHO grade 4)	ND	None	Negative
Glioblastoma (WHO grade 4)	ND	None	Negative
Glioblastoma (WHO grade 4)	ND	None	Negative

The MRS measures labeled 'ND' (not detected) were 2HG estimates \leq 0.08 mM with CRLB \geq 85%. The MRS estimates of 2HG concentrations were significantly different between mutated and wild-type *IDH* ($P = 6 \times 10^{-8}$, unpaired *t*-test).

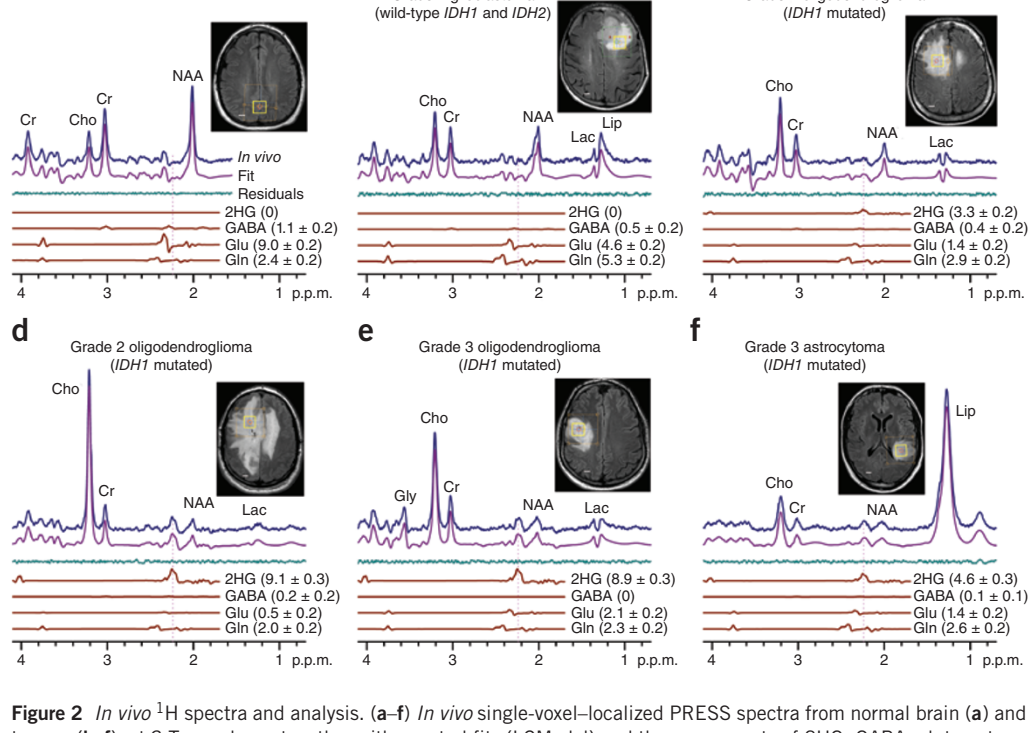


2HG detected in MRS spectra from subjects with gliomas

We included 30 subjects with gliomas in the 2HG MRS analysis (**Table 1**). The optimized PRESS was applied to the tumor mass. A representative normal brain spectrum (Fig. 2a) showed the expected pattern of choline, creatine and *N*-acetylaspartate (NAA) without evidence of 2HG. In contrast, the classic pattern of elevated choline with decreased creatine and NAA was present in all glioma grades (Fig. 2b-f). A signal attributed to 2HG was discernible at 2.25 p.p.m. in the WHO grade 2 and 3 tumors (Fig. 2c-f), but not in the glioblastoma (Fig. 2b). We identified an IDH1 or IDH2 mutation in each of these cases. We analyzed the single-voxel-localized PRESS data with linear combination of model (LCModel) software¹⁹, using spectra of 20 metabolites as basis sets, calculated incorporating the volume-localized pulses. We estimated the concentration of 2HG using the brain water signal from the voxel as reference and adjusted the relaxation effects on the observed metabolite signals using published relaxation times of brain metabolites for 3 T^{20–22}. With a 2-min scan on $2 \times 2 \times 2$ cm³ areas of brain tissue, 2HG was measurable for concentrations >1.5 mM, with Cramér-Rao lower bound (CRLB) < 18% (Table 1). With the use of precisely calculated model spectra for spectral fitting, the LCModel fits reproduced the in vivo spectra closely, resulting in residuals at the noise levels that did not show considerable chemical-shift dependences.

γ-Aminobutyric acid (GABA), glutamate and glutamine have resonances of 2.1-2.4 p.p.m. Thus, the signals are partially overlapped with the 2HG 2.25-p.p.m. signal in PRESS spectra and can interfere with 2HG estimation depending on their signal strengths. Spectral fitting with the calculated spectra enabled resolution of the metabolites with CRLB < 20% for concentrations above \sim 2 mM (**Fig. 2**). We validated the PRESS detection of 2HG using two methods. First, we compared spectral fitting outputs from a basis set with or without a 2HG signal. For spectra without measurable 2HG signals (Fig. 3a), the residuals were essentially identical between the two fitting methods. However, spectra with a noticeable signal at 2.25 p.p.m., when fitted using a basis set without 2HG, resulted in large residuals at 2.25 p.p.m. (Fig. 3a). For spectra with intermediate 2HG concentrations, the residuals were progressively larger with increasing 2HG estimates. This result shows that the signal at 2.25 p.p.m. is primarily attributable to 2HG without substantial interference from the neighboring resonances. Second, we used difference editing to confirm the PRESS measurements of 2HG in seven subjects. When a signal at 2.25 p.p.m. was discernible in PRESS spectra, we detected an edited H2 signal at 4.02 p.p.m. (Fig. 3b). When 2HG was not measurable in PRESS spectra, there was no observable edited peak at 4.02 p.p.m. (Fig. 3b). This co-detection of the PRESS 2.25 p.p.m. peak and the edited 4.02 p.p.m. signal supports the idea that the signals are both attributable to 2HG. The similarity between the 2HG concentrations a

Normal brain



C

Grade 2 oligodendroglioma

b

Grade 4 glioblastoma

Figure 2 In vivo 1 H spectra and analysis. (a–f) In vivo single-voxel–localized PRESS spectra from normal brain (a) and tumors (b–f), at 3 T, are shown together with spectral fits (LCModel) and the components of 2HG, GABA, glutamate and glutamine, as well as voxel positioning ($2 \times 2 \times 2$ cm 3). Spectra are scaled with respect to the water signal from the voxel. Vertical lines are drawn at 2.25 p.p.m. to indicate the H4 multiplet of 2HG. Shown in brackets is the estimated metabolite concentration (mM) \pm s.d. Cho, choline; Cr, creatine; Glu, glutamate; Gln, glutamine; Gly, glycine; Lac, lactate; Lip, lipids. Scale bars, 1 cm.

estimated by PRESS and editing provides evidence that the PRESS measurement of 2HG is valid, as the edited 2HG signal at 4.02 p.p.m. was generated without substantial interference from the scalar coupling connection between the 4.02 p.p.m. and $\sim\!1.9$ p.p.m. resonances, which is a unique feature of 2HG among known brain metabolites 12 .

Validation of MRS measures of 2HG by tissue analysis

We analyzed each tumor for *IDH* gene status by immunohistochemistry for the IDH1 R132H mutation and by gene sequencing of *IDH1* and *IDH2* (**Table 1**). Of the 30 subjects studied, 15 had measurable 2HG by MRS, and in each case we confirmed an *IDH1* (12 of 15 subjects) or an *IDH2* (3 of 15 subjects) mutation. The remaining 15 subjects did not have detectable 2HG by MRS (\leq 0.08 mM, CRLB > 85%), and analysis of *IDH1* and *IDH2* revealed no mutations. The MRS estimates of 2HG concentrations were significantly different between subjects with *IDH* mutations and wild-type *IDH* genes (unpaired *t*-test; $P = 6 \times 10^{-8}$).

We validated these results further by measuring D-2HG and L-2HG concentrations in tumor samples by liquid chromatography–tandem mass spectrometry (LC-MS/MS) for the 13 subjects for whom sufficient frozen material from the initial tumor resection was available (**Supplementary Table 1**). Samples from the brain tissue adjacent to tumors were available for analysis from three subjects; thus, this tissue served as relative normal controls (**Supplementary Fig. 5**). L-2HG and D-2HG were clearly differentiated in the spectra. Five wild-type *IDH1* and *IDH2* glioblastoma tumors had similar concentrations of L-2HG and D-2HG. In all tumor samples, L-2HG was <1.0 nmol per mg protein. In marked contrast, D-2HG levels in *IDH1*- and *IDH2*-mutated tumors were 20-fold to 2,000-fold higher than those in wild-type *IDH* glioblastomas (**Supplementary Fig. 6**). Taken together, these data show that

the presence of a 2HG peak in MRS is 100% correlated with the presence of a mutation in *IDH1* or *IDH2* and elevated concentrations of D-2HG in the tumor. Moreover, the absence of a 2HG peak when MRS is performed in a tumor mass is 100% correlated with wild-type *IDH1* and *IDH2* and lack of accumulation of D-2HG in the tumor tissue. Thus, the ability to detect 2HG by MRS in a tumor mass is both highly sensitive and specific.

Development of multivoxel imaging of 2HG

We extended the optimized PRESS echo time method to multivoxel imaging of 2HG. The subject with grade 3 oligodendroglioma, whose single-voxel MRS data are shown in **Figure 2e**, was scanned with 1×1 cm² resolution on a slice 1.5 cm thick that included the tumor mass (**Fig. 4a**). The patterns of the single voxel-acquired spectra were reproduced in spectra obtained with the multi-voxel MRS method. The 2HG signal at 2.25 p.p.m.

was clearly discernible in spectra from the tumor regions (Fig. 4b). Spectra from contralateral normal brain showed no 2HG signals at 2.25 p.p.m. (Fig. 4c). A map of 2HG concentrations (Fig. 4d) showed that 2HG was concentrated at the center of the T₂w-FLAIR hyperintensity region. We estimated the 2HG concentrations using the normal brain NAA concentration of 12 mM¹² as reference, giving a 2HG concentration approximately 9 mM at the center of the tumor mass, in agreement with the 2HG estimates by single-voxel MRS. The spatial distribution pattern of choline was similar to that of 2HG in the region of T₂w-FLAIR hyperintensity but, as expected, was found throughout the brain, whereas 2HG showed rapid drop off in normal brain. The NAA concentrations were low in the tumor mass, and the choline/NAA ratio in tumors was high relative to that of normal brain tissue. Because of their ability to detect 2HG in small volumes, the metabolic measures by the multivoxel MRS method may contain reduced partial-volume effects compared to the single-voxel MRS. As 2HG is unique to tumor cells, the specificity of detection is a key advance in clinical MRS for IDHmutated gliomas.

DISCUSSION

We have detected 2HG noninvasively by optimized MRS methods in subjects with gliomas and have shown concordance of 2HG levels with mutations in *IDH1* and *IDH2*, as well as accumulation of 2HG in tumor tissue. To our knowledge, this is currently the only direct metabolic consequence of a genetic mutation in a cancer cell that can be identified through noninvasive imaging. The signal overlaps of 2HG with GABA, glutamate and glutamine, which occur in short-echo-time standard data acquisitions, were overcome with multiplet narrowing by MRS sequence optimization and spectral fitting using precisely





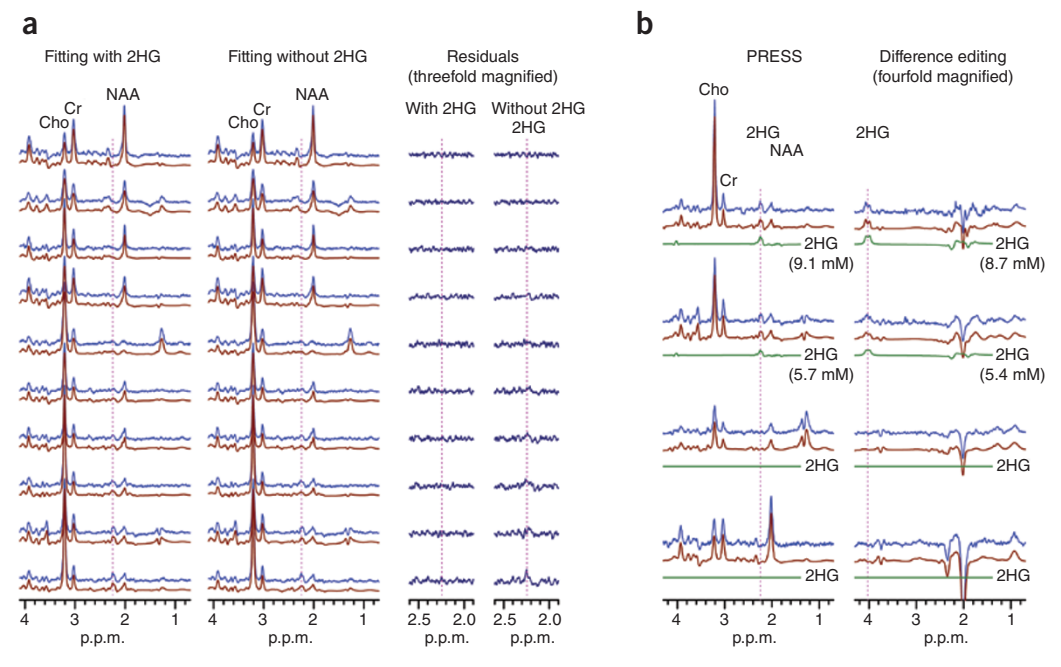


Figure 3 Validation of 2HG PRESS measurements. (a) LCModel fitting results (fits and residuals) of PRESS spectra obtained with basis set with or without 2HG. Data are displayed in order of increasing 2HG estimates, above to below. (b) PRESS and difference-edited spectra from four subjects are shown in pairs, together with LCModel fits and 2HG signal components. Vertical lines are drawn at 2.25 p.p.m. and 4.02 p.p.m. in the PRESS and edited spectra, respectively.

calculated basis spectra of metabolites. The methods presented here estimated metabolite concentrations using the brain water signal as reference in tumors, assuming an equal contribution of gray and white matter. The metabolite estimation may be valid only when the water concentration is similar among regions of the brain and between normal brain and tumor tissues. The water concentration in tumors could be increased as a result of the effects of high cellularity or brain edema, which would result in an underestimate of metabolite concentrations in the present study. Given a maximum possible water concentration of 55.6 M (bulk water), the true metabolite concentrations could be up to 30% higher than our estimates, which were obtained using a water concentration of 42.3 M, calculated from the published values for the water concentrations in gray and white matter²³. Although uncertainties in metabolite estimates can theoretically be minimized by using an

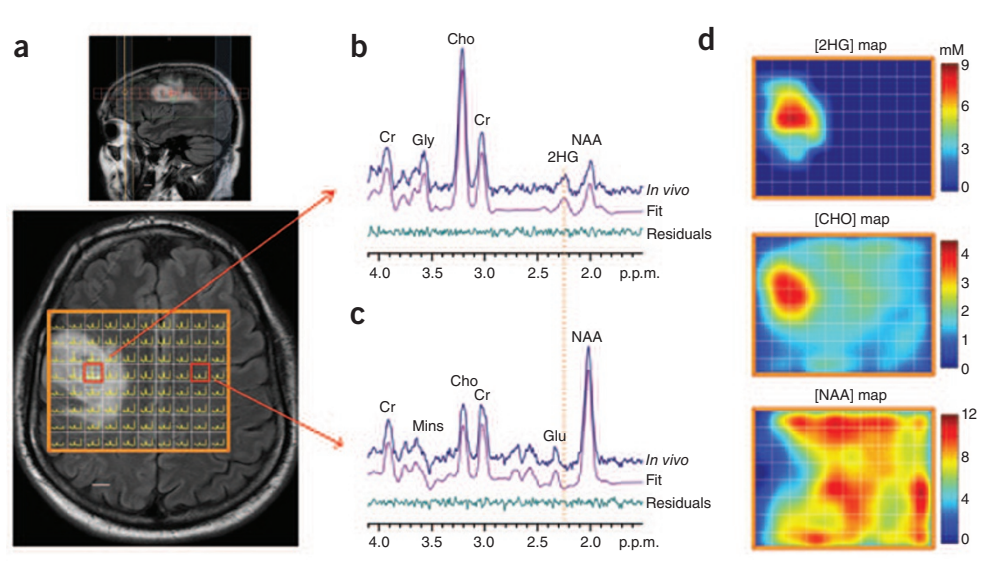
external reference signal such as from a phantom²⁴, referencing with respect to brain water signals may be a realistic means of estimating metabolite concentrations in tumors²⁵.

Two studies have previously reported in vivo detection of 2HG in the brains of people with 2-hydroxyglutaric aciduria^{26,27}. Large singlet-like signals at 2.5-2.6 p.p.m. were assigned to 2HG, although this chemical shift assignment is not consistent with in vitro highresolution magnetic resonance spectra of 2HG at neutral pH^{10} . A 2HG signal at approximately 2.5 p.p.m., which is actually a multiplet, can occur only at low pH (~2.5), as reported previously¹⁰ and confirmed in this work (Supplementary Fig. 4). The pH measured noninvasively in a wide range of tumors ranges between 6.8 and 7.2. Even using microelectrode studies, the lowest pH measured was ~6.0. An

intracellular pH of ~7.0 has been reported in cancer cells^{16–18}. The chemical shifts and coupling constants, used for MRS data analysis in the present study, were measured at pH 7.0 (ref. 10). As the proton NMR spectrum of 2HG is close to constant between pH 6.5–7.5 (**Supplementary Fig. 4**), the efficiency of detecting 2HG in gliomas should not be sensitive to tumor pH.

A PRESS sequence used for 2HG measurement in the present study is commonly available in clinical magnetic resonance systems. The field strength used here, 3 T, is becoming more commonly used in the academic and clinical magnetic resonance community, and the data-acquisition method could be implemented on standard hardware already in place in many magnetic resonance imaging centers. Without the need for more specialized instrumentation or the production of expensive exogenous probes, the detection of 2HG by MRS is a method that could

Figure 4 Spectroscopic imaging of 2HG. (a) Multivoxel imaging spectra from a subject with a WHO grade 3 oligodendroglioma are overlaid on the T₂w-FLAIR image. The grid size is 1×1 cm, with slice thickness 1.5 cm. The spectra are displayed between 4.1 p.p.m. and 1.8 p.p.m. (left to right). (**b,c**) Two representative spectra (one from the tumor and another from the contralateral normal brain) are shown together with LCModel fits and residuals. Mins, myoinositol. (d) The estimated concentrations of 2HG, choline and NAA in individual voxels were color coded for comparison. The NAA level in gray matter in normal brain was assumed to be 12 mM. Scale bars, 1 cm.



be quickly adopted for clinical use. As the presence of an *IDH1* or *IDH2* mutation makes the diagnosis of glioma when evaluating a brain mass, the ability to detect 2HG by MRS will be a valuable diagnostic tool. Although not obviating the need for a surgical procedure to determine tumor grade, the presence of 2HG on MRS would differentiate a tumor from a non-neoplastic process such as demyelinating disease. Moreover, the association of *IDH1* and *IDH2* mutations with improved survival among gliomas makes the detection of 2HG an important prognostic marker as well.

The additional clinical value of this biomarker may be in its dynamic measurement over the time course of treatment and follow up. If 2HG concentrations reflect changes in tumor cellularity, then proliferation would lead to increased 2HG concentrations, and tumor cells killed by radiation or chemotherapy would lead to decreased 2HG concentrations. Stable disease would be expected to have stable 2HG concentrations. Although these correlations are still speculative, potential clinical applications include the follow up of patients with WHO grade 2 gliomas who typically have a long period of minimal progression that is followed rapidly by aggressive growth and transformation to high grade. Similarly, the availability of an imaging biomarker to follow for the detection of recurrent disease or response to chemotherapy would be a major advance in the clinical management of patients with gliomas. Additional studies of the dynamic properties of 2HG measurement will address these potential uses.

METHODS

Methods and any associated references are available in the online version of the paper at http://www.nature.com/nm/.

Note: Supplementary information is available on the Nature Medicine website.

ACKNOWLEDGMENTS

This work was supported by US National Institutes of Health grants RC1NS0760675, R21CA159128, and RR02584 and by the Cancer Prevention Research Institute of Texas grant RP101243-P04. We thank C. Sheppard for expert management of the patient database and for coordinating research scans and tissue samples; S. McNeil for expert human subject care during scanning; C. Foong for expert assistance with pathological analysis of tumor; and R.L. Boriack for expert assistance with 2HG measurements by mass spectrometry.

AUTHOR CONTRIBUTIONS

C.C. developed the MRS methodology for 2HG detection, designed and performed the magnetic resonance experiments and data analysis, supervised the MRS study, prepared figures and wrote the manuscript. E.A.M. led all aspects of the human study, contributed to data analysis, preparation of the figures and writing of the manuscript. S.K.G. carried out magnetic resonance data acquisition and contributed to data analysis. D.R. performed mass spectrometry analysis on resected tumors and contributed to manuscript preparation. Z.K. synthesized 2HG and prepared a figure. R.J.D. and C.R.M. contributed to the conceptual approach, review of the data and manuscript preparation. K.J.H. and J.M.R. contributed to tumor sample collection and validation, neuropathological evaluation and diagnosis, evaluation of immunohistochemical stains and manuscript preparation. X.-L.Y. and T.M. performed the tissue evaluation of IDH mutations. I.M.-V. and J.M.P. contributed to conceptual analysis. B.E.M. recruited subjects and contributed to clinical data analysis and manuscript preparation. C.J.M. recruited subjects and contributed to manuscript preparation. R.M.B. contributed to the conceptual approach, led the tumor analysis workup, and contributed to data analysis and manuscript preparation.

COMPETING FINANCIAL INTERESTS

The authors declare no competing financial interests.

Published online at http://www.nature.com/naturemedicine/. Reprints and permissions information is available online at http://www.nature.com/ reprints/index.html.

- 1. Balss, J. et al. Analysis of the IDH1 codon 132 mutation in brain tumors. Acta Neuropathol. 116, 597-602 (2008).
- Yan, H. et al. IDH1 and IDH2 mutations in gliomas. N. Engl. J. Med. 360, 765-773 (2009).
- Dang, L. et al. Cancer-associated IDH1 mutations produce 2-hydroxyglutarate. Nature **462**, 739-744 (2009).
- Figueroa, M.E. et al. Leukemic IDH1 and IDH2 mutations result in a hypermethylation phenotype, disrupt TET2 function, and impair hematopoietic differentiation. Cancer Cell 18, 553-567 (2010).
- 5. Christensen, B.C. et al. DNA methylation, isocitrate dehydrogenase mutation, and survival in glioma. J. Natl. Cancer Inst. 103, 143-153 (2011).
- Parsons, D.W. et al. An integrated genomic analysis of human glioblastoma multiforme. Science 321, 1807-1812 (2008).
- von Deimling, A., Korshunov, A. & Hartmann, C. The next generation of glioma biomarkers: MGMT methylation, BRAF fusions and IDH1 mutations. Brain Pathol. 21, 74-87 (2011).
- Bottomley, P.A. Selective volume method for performing localized NMR spectroscopy. US Patent 4,480,228 (1984).
- Mescher, M., Merkle, H., Kirsch, J., Garwood, M. & Gruetter, R. Simultaneous in vivo spectral editing and water suppression. *NMR Biomed.* **11**, 266–272 (1998). 10. Bal, D. & Gryff-Keller, A. ¹H and ¹³C NMR study of 2-hydroxyglutaric acid and lactone.
- Magn. Reson. Chem. 40, 533-536 (2002).
- 11. Krawczyk, H. & Gradowska, W. Characterisation of the ¹H and ¹³C NMR spectra of N-acetylaspartylglutamate and its detection in urine from patients with Canavan disease. J. Pharm. Biomed. Anal. 31, 455-463 (2003).
- 12. Govindaraju, V., Young, K. & Maudsley, A.A. Proton NMR chemical shifts and coupling constants for brain metabolites. NMR Biomed. 13, 129-153 (2000).
- 13. Ernst, R.R., Bodenhausen, G. & Wokaun, A. Principles of nuclear magnetic resonance in one and two dimensions Ch. 2 (Clarendon Press, Oxford, UK, 1987).
- 14. Thompson, R.B. & Allen, P.S. Sources of variability in the response of coupled spins to the PRESS sequence and their potential impact on metabolite quantification. Magn. Reson. Med. 41, 1162-1169 (1999).
- 15. Choi, C. et al. Improvement of resolution for brain coupled metabolites by optimized $^1\mathrm{H}$ MRS at 7T. NMR Biomed. 23, 1044-1052 (2010).
- 16. Gillies, R.J., Raghunand, N., Garcia-Martin, M.L. & Gatenby, R.A. pH imaging. A review of pH measurement methods and applications in cancers. IEEE Eng. Med. Biol. Mag. 23, 57-64 (2004).
- 17. Griffiths, J.R. Are cancer cells acidic? Br. J. Cancer 64, 425-427 (1991).
- 18. McLean, L.A., Roscoe, J., Jorgensen, N.K., Gorin, F.A. & Cala, P.M. Malignant gliomas display altered pH regulation by NHE1 compared with nontransformed astrocytes. Am. J. Physiol. Cell Physiol. 278, C676-C688 (2000).
- 19. Provencher, S.W. Estimation of metabolite concentrations from localized in vivo proton NMR spectra. Magn. Reson. Med. 30, 672-679 (1993).
- 20. Mlynarik, V., Gruber, S. & Moser, E. Proton T (1) and T (2) relaxation times of human brain metabolites at 3 tesla. NMR Biomed. 14, 325–331 (2001).
- 21. Träber, F., Block, W., Lamerichs, R., Gieseke, J. & Schild, H.H. ¹H metabolite relaxation times at 3.0 tesla: measurements of T1 and T2 values in normal brain and determination of regional differences in transverse relaxation. J. Magn. Reson. Imaging ${f 19},\,537-545$ (2004).
- 22. Ganji, S.K. et al. T2 measurement of J-coupled metabolites in the human brain at 3T. NMR Biomed. published online, doi:10.1002/nbm.1767 (15 August 2011).
- 23. Norton, W.T., Poduslo, S.E. & Suzuki, K. Subacute sclerosing leukoencephalitis. II. Chemical studies including abnormal myelin and an abnormal ganglioside pattern. J. Neuropathol. Exp. Neurol. 25, 582-597 (1966).
- 24. Keevil, S.F. et al. Absolute metabolite quantification by in vivo NMR spectroscopy: II. A multicentre trial of protocols for in vivo localised proton studies of human brain. Magn. Reson. Imaging 16, 1093-1106 (1998).
- 25. Tong, Z., Yamaki, T., Harada, K. & Houkin, K. In vivo quantification of the metabolites in normal brain and brain tumors by proton MR spectroscopy using water as an internal standard. Magn. Reson. Imaging 22, 1017-1024 (2004).
- 26. Sener, R.N. L-2 hydroxyglutaric aciduria: proton magnetic resonance spectroscopy and diffusion magnetic resonance imaging findings. J. Comput. Assist. Tomogr. 27, 38-43
- 27. Goffette, S.M. et al. L-2-Hydroxyglutaric aciduria: clinical, genetic, and brain MRI characteristics in two adult sisters. Eur. J. Neurol. 13, 499-504 (2006).



ONLINE METHODS

Subject inclusion. We selected subjects from two University of Texas Southwestern Medical Center (UTSW) Institutional Review Board-approved brain tumor clinical protocols that have magnetic resonance imaging and include MRS as part of the study procedures. We obtained informed consent for each subject. Scans from 53 subjects were screened and were included for analysis of 2HG if (i) there was a visible tumor mass by standard magnetic resonance sequences (gadolinium enhancement or T2w-FLAIR signal abnormality), (ii) MRS had been performed in at least 1 voxel in the tumor that was of acceptable spectral quality (singlet line width <6 Hz), and (iii) there was adequate tissue available for IDH gene sequencing. Scans from 30 subjects met these criteria, and 29 subjects had been imaged before initial surgery or after a limited surgical procedure (biopsy or subtotal resection) and had not been treated with chemotherapy or radiation. One subject with secondary GBM was imaged at the time of recurrence, 3 years after treatment with radiation. A search was done in each case for the availability of frozen tissue. In 13 of 30 cases, a frozen tumor sample was identified, with three cases having both tumor and a sample of adjacent, non-tumor-bearing brain available for analysis.

Magnetic resonance spectroscopy data acquisition. Experiments were carried out on a 3-T whole-body scanner (Philips Medical Systems). A body coil was used for radiofrequency transmission and an eight-channel head coil was used for reception. Data were acquired according to our published methods²⁸. PRESS⁸ and scalar difference editing⁹ were used for measuring 2HG in brain tumors. For editing, two 20-ms Gaussian 180° pulses, tuned to 1.9 p.p.m., were switched on and off in alternate scans to generate an edited H2 signal at 4.02 p.p.m. in difference spectra. The echo times of PRESS and editing were 97 ms and 106 ms, respectively. The quantum-mechanical simulations were carried out by means of the product operator-based transformation matrix algorithm (Supplementary Methods). For in vivo magnetic resonance scans, following the survey imaging, T2w-FLAIR images were acquired to identify tumor regions. For single-voxel–localized data acquisition, a $2 \times 2 \times 2$ cm³ voxel was positioned in the tumor mass. PRESS acquisition parameters included a sweep width of 2500 Hz, 2,048 sampling points, a repetition time of 2 s, and 64 averages (scan time 2.1 min). Editing data were acquired with 384 averages (scan time 13 min). An unsuppressed water signal was acquired with an echo time of 14 ms and a repetition time of 20 s for use as a reference in metabolite quantification. Spectroscopic imaging data were acquired, using the optimized PRESS echo time, from a slice 1.5 cm thick with a resolution of 1×1 cm². We carried out undersampling of k-space data by 20%, the scan time being approximately10 min (two averages, repetition time = 1.3 s). Data were zero filled for the unacquired k-space points and filtered with a cosine function before Fourier transformation.

Magnetic resonance spectroscopy data analysis. Data were analyzed as described²⁸. Following a 1-Hz apodization, spectra were fitted with LCModel software¹⁹, using calculated spectra of 20 metabolites as basis functions. The basis set included spectra of 2HG, NAA, GABA, glutamate, glycine, creatine, myoinositol, glutamine, lactate, alanine, acetate, aspartate, ethanolamine, glutathione, phosphorylethanolamine, scyllo-inositol, taurine, N-acetylaspartylglutamate, glucose and choline. The metabolite concentrations were estimated with respect to the short-echo-time water signal. Assuming an equal composition of gray and white matter in tumors, we used a water concentration value of 42.3 M, calculated from the literature values²³ for the water concentrations in gray and white matter. Relaxation effects on metabolite signals were corrected using published metabolite T_2 and T_1 : $T_2 = 150$ ms, 230 ms and 280 ms for Cr, Cho and NAA, and 180 ms for other metabolites, respectively; $T_1 = 1.2$ ms for 2HG, glutamate, glutamine and myo-inositol, and 1.5 ms for other metabolites^{20–22}.

Immunohistochemistry for detection of the R132H mutation in *IDH1*. Paraffin sections were cut at 4-µm thickness and prepared according to standard clinical methods. The primary antibody for *IDH1* R132H (Dianova) was diluted 1 in 20.

IDH1 and *IDH2* DNA sequencing. DNA was prepared from frozen tissue by standard methods or from formalin-fixed paraffin embedded samples according to a published method²⁹. Primers for *IDH1* and *IDH2* sequencing were used according to published methods^{1,3}.

Measurement of 2HG enantiomers by mass spectrometry. D-2HG and L-2HG were extracted from tumor tissue and normal brain, and LC-MS/MS analyses were performed as described^{30,31}.

Statistical analyses. Cramér-Rao lower bounds of metabolite estimates, which represent the lower bounds of the precision, were obtained with the built-in algorithm of the LCModel software¹⁹.

Additional methods. Detailed methodology for 2HG synthesis and transformation matrix-incorporated density-matrix simulations is described in the **Supplementary Methods**.

- 28. Choi, C. *et al.* Measurement of glycine in the human brain *in vivo* by ¹H-MRS at 3 T: application in brain tumors. *Magn. Reson. Med.* **66**, 609–618 (2011).
- Maher, E.A. et al. Marked genomic differences characterize primary and secondary glioblastoma subtypes and identify two distinct molecular and clinical secondary glioblastoma entities. Cancer Res. 66, 11502–11513 (2006).
- Rakheja, D., Mitui, M., Boriack, R.L. & DeBerardinis, R.J. Isocitrate dehydrogenase 1/2
 mutational analyses and 2-hydroxyglutarate measurements in Wilms tumors. *Pediatr. Blood Cancer* 56, 379–383 (2011).
- Rakheja, D. et al. Papillary thyroid carcinoma shows elevated levels of 2-hydroxyglutarate. Tumour Biol. 32, 325–333 (2011).

NATURE MEDICINE doi:10.1038/nm.2682